Cell Reports Medicine, Volume *5*

Supplemental information

Targeting MCL1-driven anti-apoptotic pathways overcomes blast progression after hypomethylating agent failure in chronic myelomonocytic leukemia

Guillermo Montalban-Bravo, Natthakan Thongon, Juan Jose Rodriguez-Sevilla, Feiyang Ma, Irene Ganan-Gomez, Hui Yang, Yi June Kim, Vera Adema, Bethany Wildeman, Tomoyuki Tanaka, Faezeh Darbaniyan, Gheath Al-Atrash, Karen Dwyer, Sanam Loghavi, Rashmi Kanagal-Shamanna, Xingzhi Song, Jianhua Zhang, Koichi Takahashi, Hagop Kantarjian, Guillermo Garcia-Manero, and Simona Colla

A

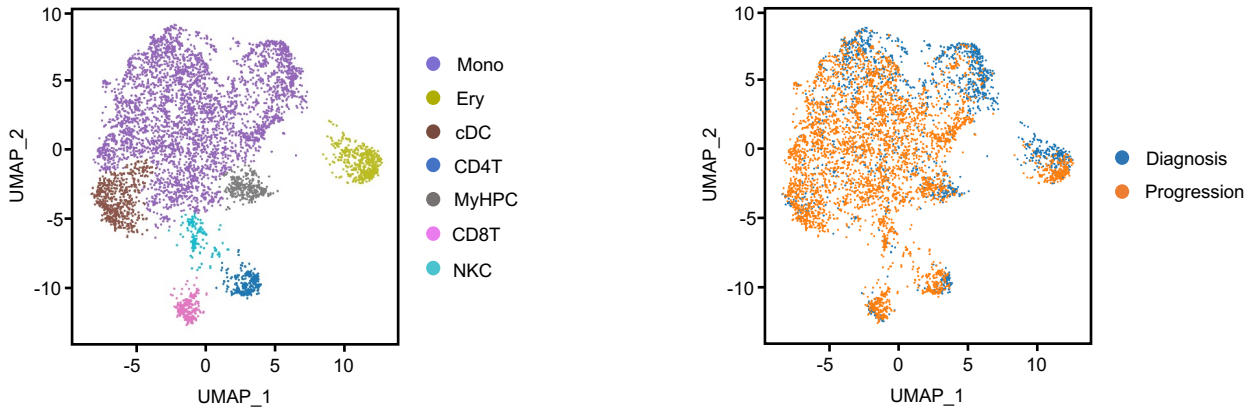
UMAP_2
UMAP_1
Mono
Ery
cDC
CD4T
MyHPC
CD8T
NKC
Diagnosis
Progression

B

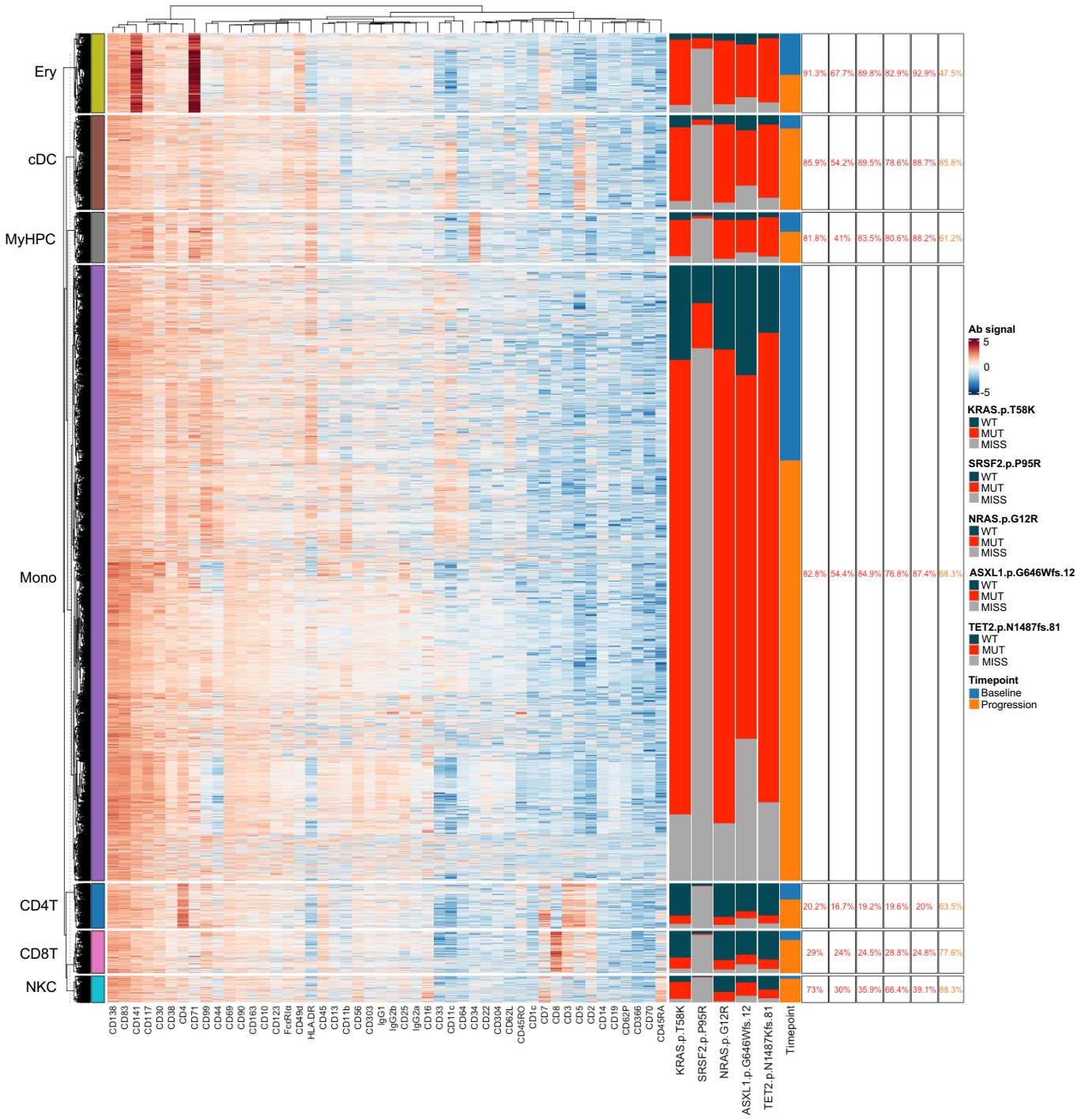
Ery
cDC
MyHPC
Mono
CD4T
CD8T
NKC
91.3% 67.7% 89.8% 82.9% 92.9% 47.5%
85.9% 54.2% 89.5% 78.6% 88.7% 85.8%
81.8% 41% 83.5% 80.6% 88.2% 61.2%
82.8% 54.4% 84.9% 76.8% 87.4% 68.3%
20.2% 16.7% 19.2% 19.6% 20% 63.5%
29% 24% 24.5% 28.8% 24.8% 77.6%
73% 30% 35.9% 66.4% 39.1% 88.3%
CD138 CD83 CD141 CD117 CD30 CD38 CD34 CD71 CD99 CD44 CD69 CD90 CD163 CD10 CD123 FcεRIα CD49d HLADR CD45 CD13 CD11b CD56 CD303 IgG1 IgG2b CD25 IgG2a CD16 CD33 CD11c CD64 CD34 CD22 CD304 CD62L CD45RO CD1c CD7 CD8 CD3 CD5 CD2 CD14 CD19 CD62P CD366 CD70 CD45RA
KRAS.p.T58K SRSF2.p.P95R NRAS.p.G12R ASXL1.p.G646Wfs.12 TET2.p.N1487fs.81 Timepoint
Ab signal
5
0
-5
KRAS.p.T58K
WT
MUT
MISS
SRSF2.p.P95R
WT
MUT
MISS
NRAS.p.G12R
WT
MUT
MISS
ASXL1.p.G646Wfs.12
WT
MUT
MISS
TET2.p.N1487fs.81
WT
MUT
MISS
Timepoint
Baseline
Progression

Figure S1. Mutations in *RAS* pathway signaling genes predict a high risk of CMML BP after HMA therapy failure. Related to Figure 1. (A) UMAP of scDNA and protein-seq data for pooled MNCs isolated from BM samples obtained from a CMML patient with pre-existing $KRAS^{T58K}$ and $NRAS^{G12R}$ mutations at diagnosis (n=1,826) and at BP after HMA therapy failure (n=4,001) included in the CMML patient cohort in Figure 1 and evaluated patient samples in Figure 4. BP was not associated with the clonal evolution of these mutations as they both had approximately 50% VAF at the onset of the disease. Each dot represents one cell. Cells are clustered based on immunophenotypic markers. Different colors represent cluster identity (left) or origin (right). Mono, monocytes; Ery, erythroid precursors; cDC, classical dendritic cells; CD4T, $CD4^+$ T cells; MyHPC, myeloid hematopoietic progenitor cells; CD8T, $CD8^+$ T cells; NKC, natural killer cells. **(B)** Heatmap displaying DNA and protein reads from each sequenced cell type shown in Fig. S1A. Colors for protein data correspond to antibody-oligonucleotide intensity signals. High protein expression is depicted in red, and low protein expression is depicted in blue. DNA colors correspond to the genotypes for each individual mutation per cell read (wild-type = dark grey, mutant = red, missing = light grey) based on cluster. Percentages correspond to the frequencies of mutant reads within each cluster for a given mutation.

A

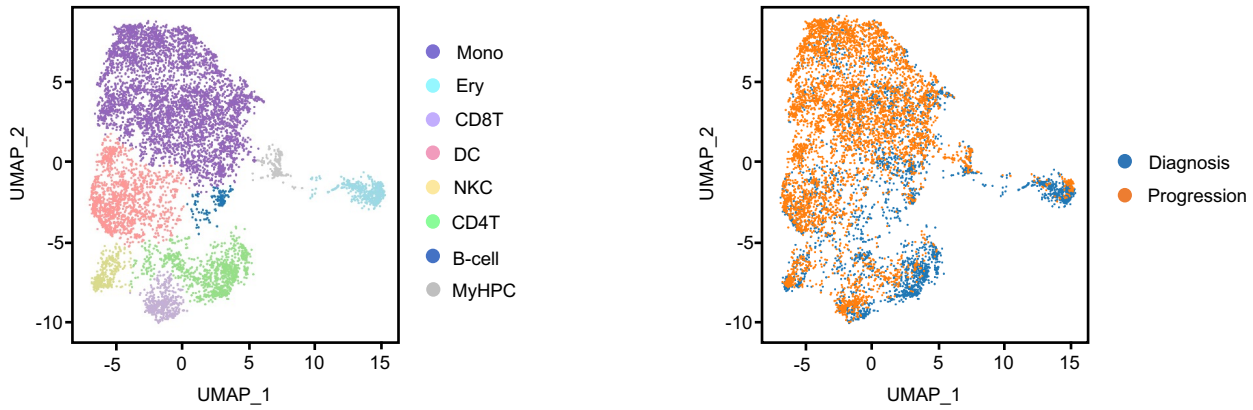
UMAP_2
UMAP_1
Mono
Ery
CD8T
DC
NKC
CD4T
B-cell
MyHPC
Diagnosis
Progression

B

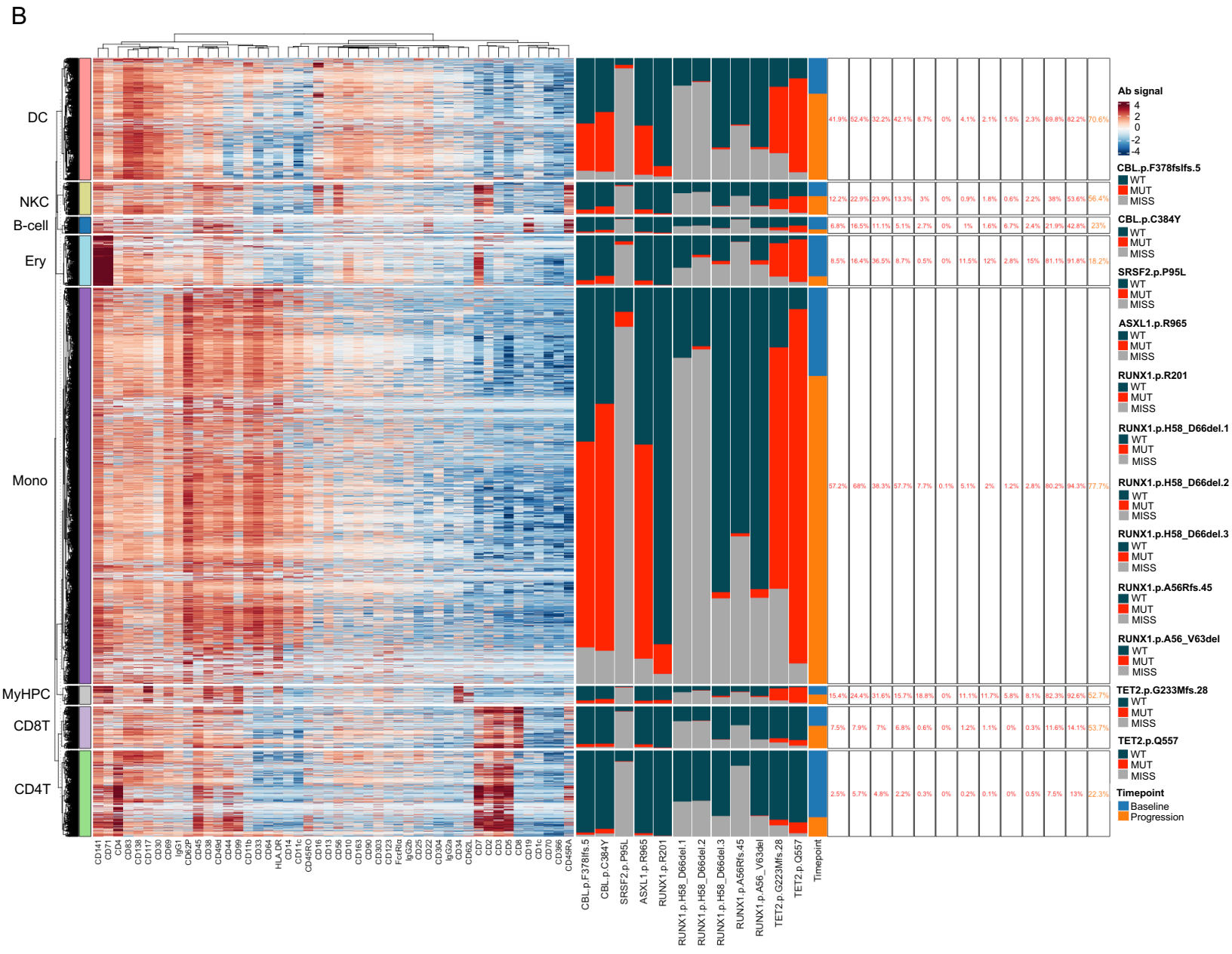
DC
NKC
B-cell
Ery
Mono
MyHPC
CD8T
CD4T
Ab signal
CBL.p.F378fslfs.5
CBL.p.C384Y
SRSF2.p.P95L
ASXL1.p.R965
RUNX1.p.R201
RUNX1.p.H58_D66del.1
RUNX1.p.H58_D66del.2
RUNX1.p.H58_D66del.3
RUNX1.p.A56Rfs.45
RUNX1.p.A56_V63del
TET2.p.G233Mfs.28
TET2.p.Q557
Timepoint
WT
MUT
MISS
Baseline
Progression

Figure S2. *RAS* pathway mutant clones expand at BP after HMA therapy failure in CMML. Related to Figure 1. (A) UMAP of scDNA and protein-seq data for pooled MNCs isolated from BM samples obtained from a CMML patient at diagnosis (n=3,213) and at BP after HMA therapy failure (n=5,342) included in the CMML patient cohort in Figure 1 and evaluated patient samples in Figure 4. BP was associated with the clonal evolution of a pre-existing $CBL^{F378Ifs}$ mutation and the acquisition of a previously undetected CBL^{C384Y} mutation. Each dot represents one cell. Cells are clustered based on immunophenotypic markers. Different colors represent cluster identity (left) or origin (right). Mono, monocytes; Ery, erythroid precursors; CD8T, $CD8^+$ T cells; DC, classical dendritic cells; NKC, natural killer cells; CD4T, $CD4^+$ T cells; B cell, B lymphocytes, MyHPC; myeloid hematopoietic progenitor cells. **(B)** Heatmap displaying DNA and protein reads from each sequenced cell type as shown in Fig. S2A. Colors for protein data correspond to antibody-oligonucleotide intensity signals. Red indicates high protein expression, and blue indicates low protein expression. Colors for DNA data correspond to the genotype for each individual mutation per cell read (wild-type = dark grey, mutant = red, missing = light grey) based on cluster. Percentages correspond to the frequencies of mutant reads within each cluster for a given mutation.

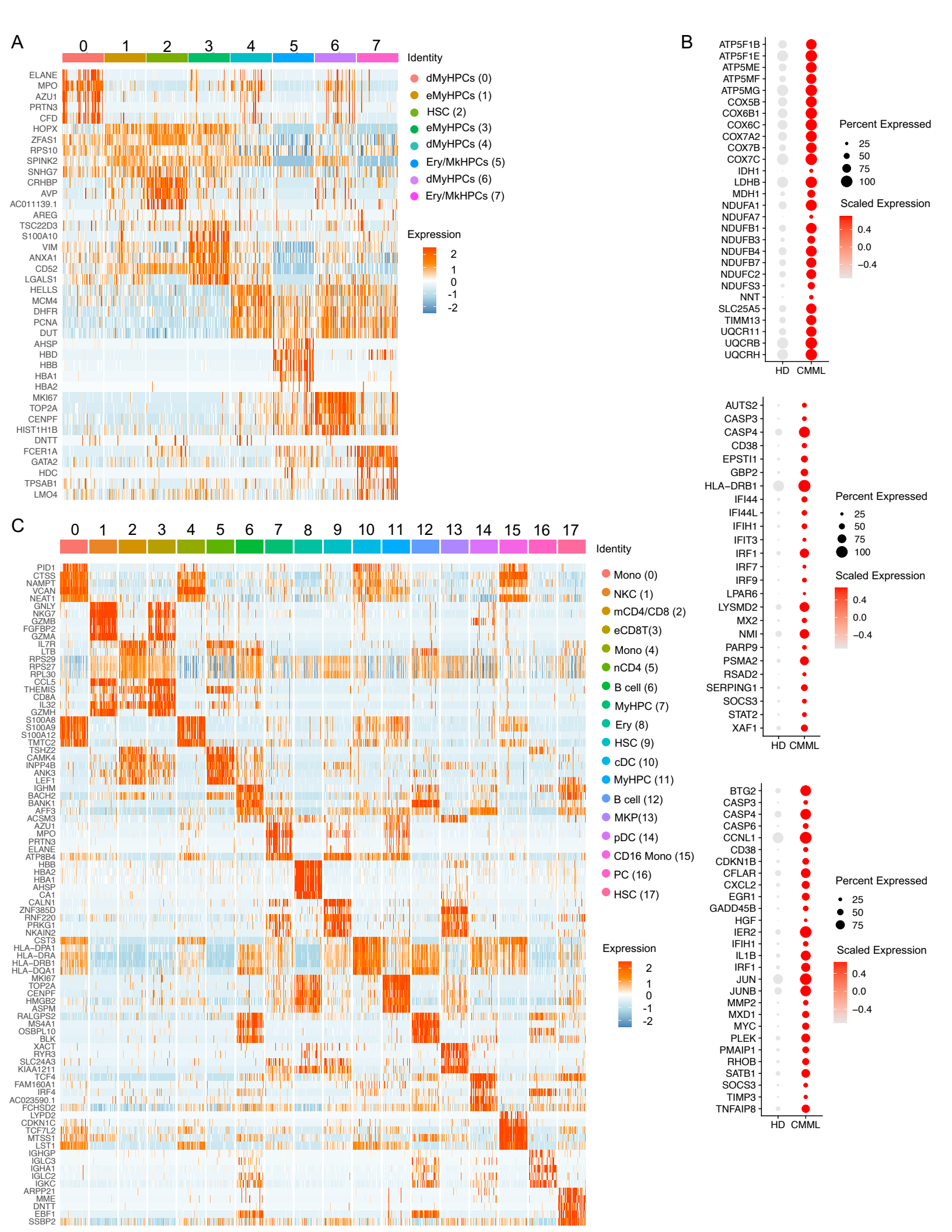
A
0 1 2 3 4 5 6 7
ELANE
MPO
AZU1
PRTN3
CFD
HOPX
ZFAS1
RPS10
SPINK2
SNHG7
CRHBP
AVP
AC011139.1
AREG
TSC22D3
S100A10
VIM
ANXA1
CD52
LGALS1
HELLS
MCM4
DHFR
PCNA
DUT
AHSP
HBD
HBB
HBA1
HBA2
MKI67
TOP2A
CENPF
HIST1H1B
DNTT
FCER1A
GATA2
HDC
TPSAB1
LMO4
Identity
dMyHPCs (0)
eMyHPCs (1)
HSC (2)
eMyHPCs (3)
dMyHPCs (4)
Ery/MkHPCs (5)
dMyHPCs (6)
Ery/MkHPCs (7)
Expression
2
1
0
-1
-2
B
ATP5F1B
ATP5F1E
ATP5ME
ATP5MF
ATP5MG
COX5B
COX6B1
COX6C
COX7A2
COX7B
COX7C
IDH1
LDHB
MDH1
NDUFA1
NDUFA7
NDUFB1
NDUFB3
NDUFB4
NDUFB7
NDUFC2
NDUFS3
NNT
SLC25A5
TIMM13
UQCR11
UQCRB
UQCRH
HD CMML
Percent Expressed
25
50
75
100
Scaled Expression
0.4
0.0
−0.4
AUTS2
CASP3
CASP4
CD38
EPSTI1
GBP2
HLA−DRB1
IFI44
IFI44L
IFIH1
IFIT3
IRF1
IRF7
IRF9
LPAR6
LYSMD2
MX2
NMI
PARP9
PSMA2
RSAD2
SERPING1
SOCS3
STAT2
XAF1
HD CMML
Percent Expressed
25
50
75
100
Scaled Expression
0.4
0.0
−0.4
BTG2
CASP3
CASP4
CASP6
CCNL1
CD38
CDKN1B
CFLAR
CXCL2
EGR1
GADD45B
HGF
IER2
IFIH1
IL1B
IRF1
JUN
JUNB
MMP2
MXD1
MYC
PLEK
PMAIP1
RHOB
SATB1
SOCS3
TIMP3
TNFAIP8
HD CMML
Percent Expressed
25
50
75
Scaled Expression
0.4
0.0
−0.4
C
0 1 2 3 4 5 6 7 8 9 10 11 12 13 14 15 16 17
PID1
CTSS
NAMPT
VCAN
NEAT1
GNLY
NKG7
GZMB
FGFBP2
GZMA
IL7R
LTB
RPS29
RPS27
RPL30
CCL5
THEMIS
CD8A
IL32
GZMH
S100A8
S100A9
S100A12
TMTC2
TSHZ2
CAMK4
INPP4B
ANK3
LEF1
IGHM
BACH2
BANK1
AFF3
ACSM3
AZU1
MPO
PRTN3
ELANE
ATP8B4
HBB
HBA2
HBA1
AHSP
CA1
CALN1
ZNF385D
RNF220
PRKG1
NKAIN2
CST3
HLA−DPA1
HLA−DRA
HLA−DRB1
HLA−DQA1
MKI67
TOP2A
CENPF
HMGB2
ASPM
RALGPS2
MS4A1
OSBPL10
BLK
XACT
RYR3
SLC24A3
KIAA1211
TCF4
FAM160A1
IRF4
AC023590.1
FCHSD2
LYPD2
CDKN1C
TCF7L2
MTSS1
LST1
IGHGP
IGLC3
IGHA1
IGLC2
IGKC
ARPP21
MME
DNTT
EBF1
SSBP2
Identity
Mono (0)
NKC (1)
mCD4/CD8 (2)
eCD8T(3)
Mono (4)
nCD4 (5)
B cell (6)
MyHPC (7)
Ery (8)
HSC (9)
cDC (10)
MyHPC (11)
B cell (12)
MKP(13)
pDC (14)
CD16 Mono (15)
PC (16)
HSC (17)
Expression
2
1
0
-1
-2

Figure S3. *RAS* pathway mutated CMML cells activate cell-intrinsic and -extrinsic inflammatory networks. Related to Figure 2. **(A)** Heatmap of the expression levels of the top 5 genes enriched in each of the 8 clusters shown in Fig. 2A. **(B)** Dot plots of the genes belonging to oxidative phosphorylation (top), IFN response (middle), and apoptosis (bottom) pathways that were significantly overexpressed in the CMML HSCs shown in Fig. 2A compared with those in HD HSCs. The scaled expression represents z scores across conditions. **(C)** Heatmap of the expression levels of the top 5 genes enriched in each of the 18 clusters shown in Fig. 2D.

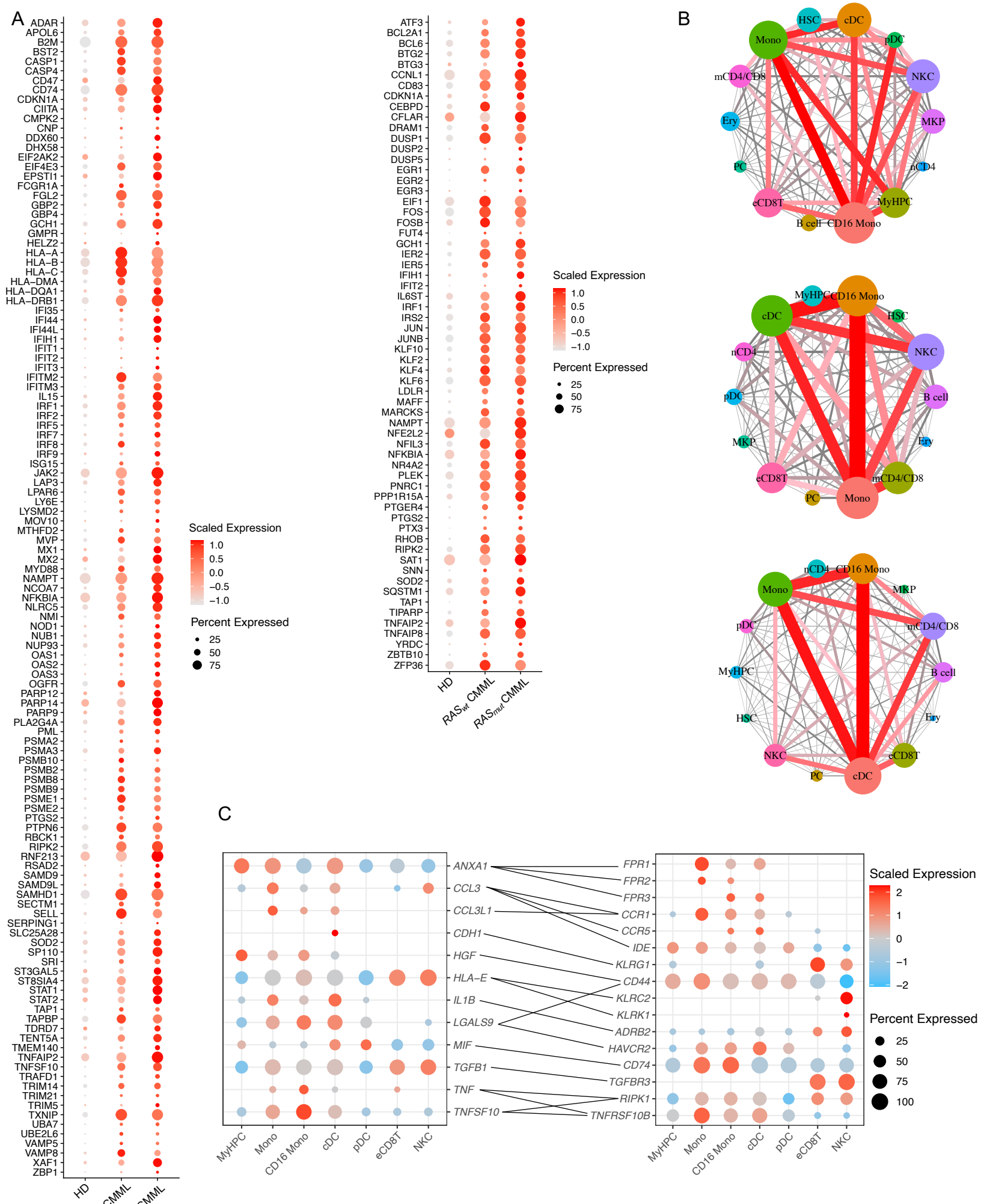
A
ADAR
APOL6
B2M
BST2
CASP1
CASP4
CD47
CD74
CDKN1A
CIITA
CMPK2
CNP
DDX60
DHX58
EIF2AK2
EIF4E3
EPSTI1
FCGR1A
FGL2
GBP2
GBP4
GCH1
GMPR
HELZ2
HLA–A
HLA–B
HLA–C
HLA–DMA
HLA–DQA1
HLA–DRB1
IFI35
IFI44
IFI44L
IFIH1
IFIT1
IFIT2
IFIT3
IFITM2
IFITM3
IL15
IRF1
IRF2
IRF5
IRF7
IRF8
IRF9
ISG15
JAK2
LAP3
LPAR6
LY6E
LYSMD2
MOV10
MTHFD2
MVP
MX1
MX2
MYD88
NAMPT
NCOA7
NFKBIA
NLRC5
NMI
NOD1
NUB1
NUP93
OAS1
OAS2
OAS3
OGFR
PARP12
PARP14
PARP9
PLA2G4A
PML
PSMA2
PSMA3
PSMB10
PSMB2
PSMB8
PSMB9
PSME1
PSME2
PTGS2
PTPN6
RBCK1
RIPK2
RNF213
RSAD2
SAMD9
SAMD9L
SAMHD1
SECTM1
SELL
SERPING1
SLC25A28
SOD2
SP110
SRI
ST3GAL5
ST8SIA4
STAT1
STAT2
TAP1
TAPBP
TDRD7
TENT5A
TMEM140
TNFAIP2
TNFSF10
TRAFD1
TRIM14
TRIM21
TRIM5
TXNIP
UBA7
UBE2L6
VAMP5
VAMP8
XAF1
ZBP1
HD
RASwt CMML
RASmut CMML
ATF3
BCL2A1
BCL6
BTG2
BTG3
CCNL1
CD83
CDKN1A
CEBPD
CFLAR
DRAM1
DUSP1
DUSP2
DUSP5
EGR1
EGR2
EGR3
EIF1
FOS
FOSB
FUT4
GCH1
IER2
IER5
IFIH1
IFIT2
IL6ST
IRF1
IRS2
JUN
JUNB
KLF10
KLF2
KLF4
KLF6
LDLR
MAFF
MARCKS
NAMPT
NFE2L2
NFIL3
NFKBIA
NR4A2
PLEK
PNRC1
PPP1R15A
PTGER4
PTGS2
PTX3
RHOB
RIPK2
SAT1
SNN
SOD2
SQSTM1
TAP1
TIPARP
TNFAIP2
TNFAIP8
YRDC
ZBTB10
ZFP36
HD
RASwt CMML
RASmut CMML
Scaled Expression
1.0
0.5
0.0
−0.5
−1.0
Percent Expressed
25
50
75
B
HSC
cDC
Mono
pDC
mCD4/CD8
NKC
Ery
MKP
PC
nCD4
eCD8T
MyHPC
B cell
CD16 Mono
MyHPC
CD16 Mono
cDC
HSC
nCD4
NKC
pDC
B cell
MKP
Ery
eCD8T
mCD4/CD8
PC
Mono
nCD4
CD16 Mono
Mono
MKP
pDC
mCD4/CD8
MyHPC
B cell
HSC
Ery
NKC
eCD8T
PC
cDC
C
ANXA1
CCL3
CCL3L1
CDH1
HGF
HLA–E
IL1B
LGALS9
MIF
TGFB1
TNF
TNFSF10
FPR1
FPR2
FPR3
CCR1
CCR5
IDE
KLRG1
CD44
KLRC2
KLRK1
ADRB2
HAVCR2
CD74
TGFBR3
RIPK1
TNFRSF10B
MyHPC
Mono
CD16 Mono
cDC
pDC
eCD8T
NKC
Scaled Expression
2
1
0
−1
−2
Percent Expressed
25
50
75
100

Figure S4. *RAS* pathway mutated CMML cells activate inflammatory networks and establish inhibitory immune interactions. Related to Figure 2. (A) Dot plots of the genes belonging to IFN response (left) and NF-κB signaling (right) pathways that were significantly overexpressed in *RAS* pathway mutant and/or wild-type CMML monocytes shown in Fig. 2D compared with those in HD monocytes. The scaled expression represents z scores across conditions. **(B)** Connectome web analysis of interactions between BM MNC populations that were significantly increased in *RAS* pathway wild-type (top) or mutant (middle) CMML compared to those of HDs, or in *RAS* pathway mutant CMML compared to *RAS* pathway wild-type CMML (bottom). The vertex (i.e., colored cell node) size is proportional to the number of interactions to and from each cell type, and the thickness of each connecting line is proportional to the number of interactions between 2 nodes. **(C)** Dot plots showing the most significant ligand- (left) to-receptor (right) interactions gained in MNCs from *RAS* pathway mutant CMML patients compared with those from *RAS* pathway wild-type CMML. Lines represent connections between ligands and their corresponding receptors. Color saturation indicates the level of gene expression. Dot size indicates the percentage of each cell type expressing the gene. The scaled expression represents z scores across conditions.

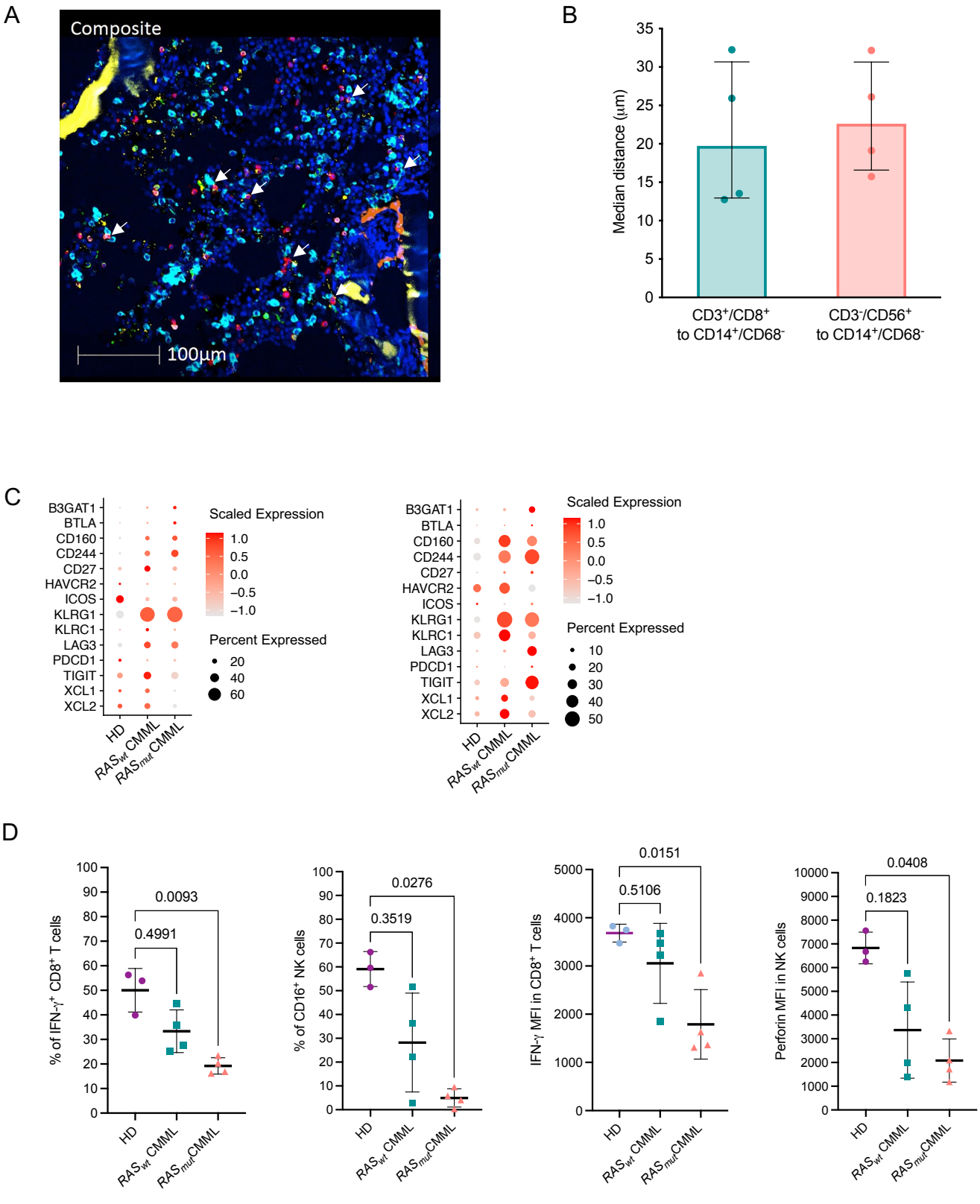
A
Composite
100µm
B
Median distance (µm)
CD3+/CD8+ to CD14+/CD68-
CD3-/CD56+ to CD14+/CD68-
C
B3GAT1
BTLA
CD160
CD244
CD27
HAVCR2
ICOS
KLRG1
KLRC1
LAG3
PDCD1
TIGIT
XCL1
XCL2
Scaled Expression
Percent Expressed
HD
RASwt CMML
RASmut CMML
D
% of IFN-γ+ CD8+ T cells
% of CD16+ NK cells
IFN-γ MFI in CD8+ T cells
Perforin MFI in NK cells
0.0093
0.4991
0.0276
0.3519
0.0151
0.5106
0.0408
0.1823

Figure S5. Immune cells are in a dysfunctional state in CMML and spatially co-localize with monocytic populations. Related to Figure 2. (A) Representative multiplex immunofluorescence image of a selected BM section area (20× magnification). Cells were stained with antibodies against CD3 (red), CD4 (green), CD8 (magenta), CD14 (cyan), CD56 (orange), and CD68 (yellow). White arrows indicate the interactions between $CD14^+$ monocytes and $CD3^+$ T cells. **(B)** The median distance between $CD14^+/CD68^-$ monocytes and $CD3^+/CD8^+$ T cells (left) or $CD3^-/CD56^+$ NK cells (right) in BM sections obtained from CMML patients (n=4) at the time of diagnosis. **(C)** Dot plot of exhaustion markers in effector $CD8^+$ T (left) and NK (right) cells from HDs, and *RAS* pathway wild-type (RAS_{wt}) or mutant (RAS_{mut}) CMML. The scaled expression represents z scores across conditions. **(D)** Frequencies of IFN-γ^+ $CD8^+$ T cells (far left), $CD16^+$ NK cells (middle left), and mean fluorescent intensity (MFI) of IFN-γ^+ in $CD8^+$ T cells (middle right) or perforin in NK cells (far right) from the BM of HDs (n=3) and *RAS* pathway wild-type (RAS_{wt}) or mutant (RAS_{mut}) CMML (n=4). Lines represent means. Statistical significance was calculated using the Kruskal-Wallis test.

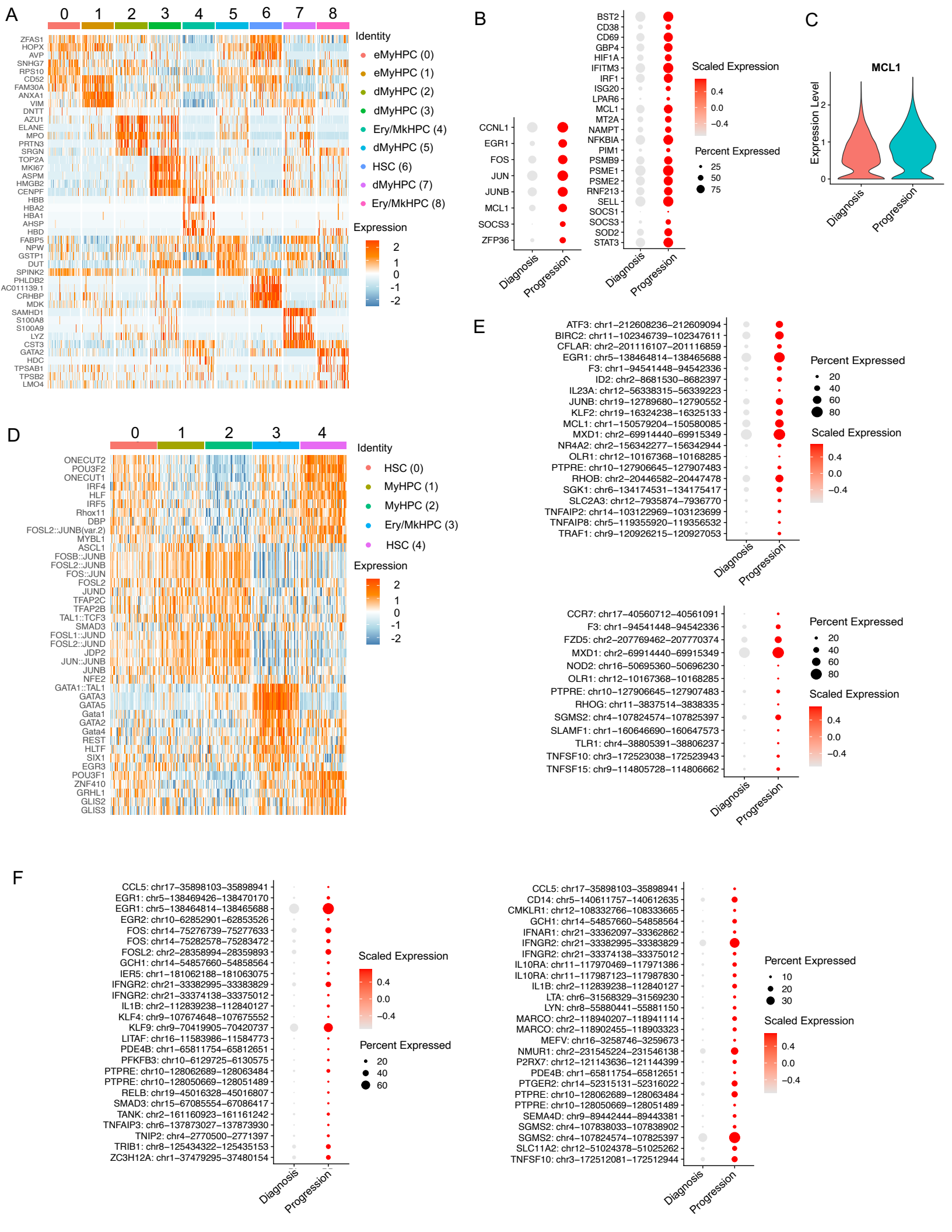
A
0 1 2 3 4 5 6 7 8
ZFAS1
HOPX
AVP
SNHG7
RPS10
CD52
FAM30A
ANXA1
VIM
DNTT
AZU1
ELANE
MPO
PRTN3
SRGN
TOP2A
MKI67
ASPM
HMGB2
CENPF
HBB
HBA2
HBA1
AHSP
HBD
FABP5
NPW
GSTP1
DUT
SPINK2
PHLDB2
AC011139.1
CRHBP
MDK
SAMHD1
S100A8
S100A9
LYZ
CST3
GATA2
HDC
TPSAB1
TPSB2
LMO4
Identity
eMyHPC (0)
eMyHPC (1)
dMyHPC (2)
dMyHPC (3)
Ery/MkHPC (4)
dMyHPC (5)
HSC (6)
dMyHPC (7)
Ery/MkHPC (8)
Expression
2
1
0
-1
-2
B
BST2
CD38
CD69
GBP4
HIF1A
IFITM3
IRF1
ISG20
LPAR6
MCL1
MT2A
NAMPT
NFKBIA
PIM1
PSMB9
PSME1
PSME2
RNF213
SELL
SOCS1
SOCS3
SOD2
STAT3
CCNL1
EGR1
FOS
JUN
JUNB
MCL1
SOCS3
ZFP36
Diagnosis
Progression
Scaled Expression
0.4
0.0
−0.4
Percent Expressed
25
50
75
C
MCL1
Expression Level
2
1
0
Diagnosis
Progression
D
0 1 2 3 4
ONECUT2
POU3F2
ONECUT1
IRF4
HLF
IRF5
Rhox11
DBP
FOSL2::JUNB(var.2)
MYBL1
ASCL1
FOSB::JUNB
FOSL2::JUNB
FOS::JUN
FOSL2
JUND
TFAP2C
TFAP2B
TAL1::TCF3
SMAD3
FOSL1::JUND
FOSL2::JUND
JDP2
JUN::JUNB
JUNB
NFE2
GATA1::TAL1
GATA3
GATA5
Gata1
GATA2
Gata4
REST
HLTF
SIX1
EGR3
POU3F1
ZNF410
GRHL1
GLIS2
GLIS3
Identity
HSC (0)
MyHPC (1)
MyHPC (2)
Ery/MkHPC (3)
HSC (4)
Expression
2
1
0
-1
-2
E
ATF3: chr1−212608236−212609094
BIRC2: chr11−102346739−102347611
CFLAR: chr2−201116107−201116859
EGR1: chr5−138464814−138465688
F3: chr1−94541448−94542336
ID2: chr2−8681530−8682397
IL23A: chr12−56338315−56339223
JUNB: chr19−12789680−12790552
KLF2: chr19−16324238−16325133
MCL1: chr1−150579204−150580085
MXD1: chr2−69914440−69915349
NR4A2: chr2−156342277−156342944
OLR1: chr12−10167368−10168285
PTPRE: chr10−127906645−127907483
RHOB: chr2−20446582−20447478
SGK1: chr6−134174531−134175417
SLC2A3: chr12−7935874−7936770
TNFAIP2: chr14−103122969−103123699
TNFAIP8: chr5−119355920−119356532
TRAF1: chr9−120926215−120927053
Diagnosis
Progression
Percent Expressed
20
40
60
80
Scaled Expression
0.4
0.0
−0.4
CCR7: chr17−40560712−40561091
F3: chr1−94541448−94542336
FZD5: chr2−207769462−207770374
MXD1: chr2−69914440−69915349
NOD2: chr16−50695360−50696230
OLR1: chr12−10167368−10168285
PTPRE: chr10−127906645−127907483
RHOG: chr11−3837514−3838335
SGMS2: chr4−107824574−107825397
SLAMF1: chr1−160646690−160647573
TLR1: chr4−38805391−38806237
TNFSF10: chr3−172523038−172523943
TNFSF15: chr9−114805728−114806662
Diagnosis
Progression
Percent Expressed
20
40
60
80
Scaled Expression
0.4
0.0
−0.4
F
CCL5: chr17−35898103−35898941
EGR1: chr5−138469426−138470170
EGR1: chr5−138464814−138465688
EGR2: chr10−62852901−62853526
FOS: chr14−75276739−75277633
FOS: chr14−75282578−75283472
FOSL2: chr2−28358994−28359893
GCH1: chr14−54857660−54858564
IER5: chr1−181062188−181063075
IFNGR2: chr21−33382995−33383829
IFNGR2: chr21−33374138−33375012
IL1B: chr2−112839238−112840127
KLF4: chr9−107674648−107675552
KLF9: chr9−70419905−70420737
LITAF: chr16−11583986−11584773
PDE4B: chr1−65811754−65812651
PFKFB3: chr10−6129725−6130575
PTPRE: chr10−128062689−128063484
PTPRE: chr10−128050669−128051489
RELB: chr19−45016328−45016807
SMAD3: chr15−67085554−67086417
TANK: chr2−161160923−161161242
TNFAIP3: chr6−137873027−137873930
TNIP2: chr4−2770500−2771397
TRIB1: chr8−125434322−125435153
ZC3H12A: chr1−37479295−37480154
Diagnosis
Progression
Scaled Expression
0.4
0.0
−0.4
Percent Expressed
20
40
60
CCL5: chr17−35898103−35898941
CD14: chr5−140611757−140612635
CMKLR1: chr12−108332766−108333665
GCH1: chr14−54857660−54858564
IFNAR1: chr21−33362097−33362862
IFNGR2: chr21−33382995−33383829
IFNGR2: chr21−33374138−33375012
IL10RA: chr11−117970469−117971386
IL10RA: chr11−117987123−117987830
IL1B: chr2−112839238−112840127
LTA: chr6−31568329−31569230
LYN: chr8−55880441−55881150
MARCO: chr2−118940207−118941114
MARCO: chr2−118902455−118903323
MEFV: chr16−3258746−3259673
NMUR1: chr2−231545224−231546138
P2RX7: chr12−121143636−121144399
PDE4B: chr1−65811754−65812651
PTGER2: chr14−52315131−52316022
PTPRE: chr10−128062689−128063484
PTPRE: chr10−128050669−128051489
SEMA4D: chr9−89442444−89443381
SGMS2: chr4−107838033−107838902
SGMS2: chr4−107824574−107825397
SLC11A2: chr12−51024378−51025262
TNFSF10: chr3−172512081−172512944
Diagnosis
Progression
Percent Expressed
10
20
30
Scaled Expression
0.4
0.0
−0.4

Figure S6. *RAS* pathway–mutated HSCs undergo epigenetic reprogramming and drive CMML BP after HMA therapy failure. Related to Figure 3. (A) Heatmap of the expression levels of the top 5 genes enriched in each of the 9 clusters shown in Fig. 3A. **(B)** Dot plots of genes belonging to the NF-κB signaling pathway that were significantly upregulated in *RAS* mutant CMML HSCs (left) and eMyHPCs (right) at BP compared with those at diagnosis (adjusted $P \leq 0.05$). The scaled expression represents z scores across conditions. **(C)** Violin plots of *MCL1* expression levels of *RAS* pathway mutant CMML HSCs at diagnosis and BP (adjusted $P = 2.55 \times 10^{-4}$). **(D)** Heatmap of the activity of the top 10 TFs enriched in each of the 5 clusters shown in Fig. 3D. **(E)** Dot plots of genes involved in the NF-$_K$B signaling (top) or inflammatory response (bottom) pathways whose promoters had increased open chromatin peaks in CMML HSCs at BP compared with those at diagnosis ($P \leq 10^{-4}$). The scaled expression represents z scores across conditions. **(F)** Dot plots of genes involved in the NF-$_K$B signaling (left) or inflammatory response (right) pathways whose distal regulatory elements had increased open chromatin peaks in CMML HSCs at BP compared with those at diagnosis (adjusted $P \leq 0.05$). The scaled expression represents z scores across conditions.

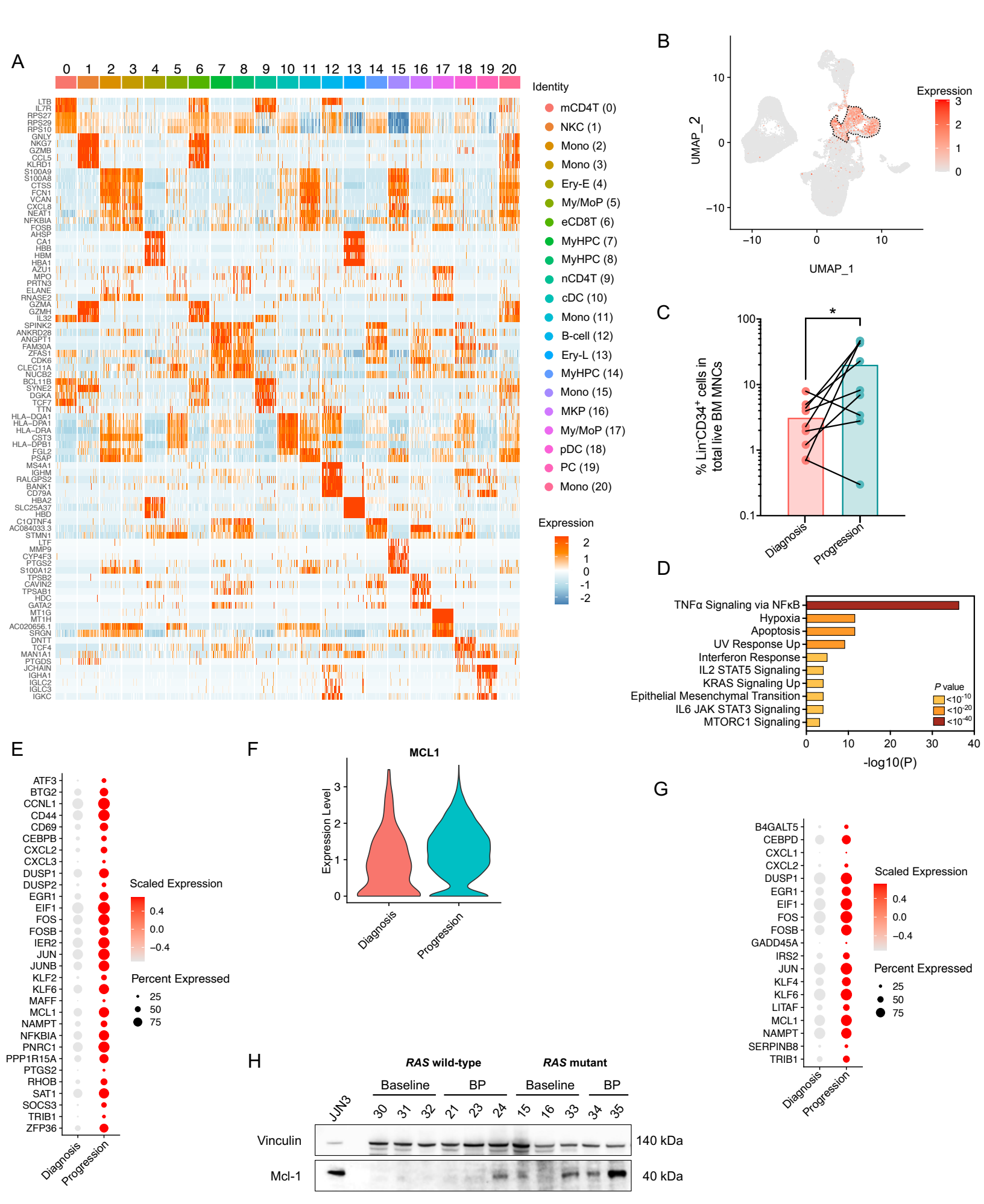
A
0 1 2 3 4 5 6 7 8 9 10 11 12 13 14 15 16 17 18 19 20
Identity
mCD4T (0)
NKC (1)
Mono (2)
Mono (3)
Ery-E (4)
My/MoP (5)
eCD8T (6)
MyHPC (7)
MyHPC (8)
nCD4T (9)
cDC (10)
Mono (11)
B-cell (12)
Ery-L (13)
MyHPC (14)
Mono (15)
MKP (16)
My/MoP (17)
pDC (18)
PC (19)
Mono (20)
Expression
2
1
0
-1
-2
B
UMAP_2
UMAP_1
Expression
3
2
1
0
C
% Lin-CD34+ cells in total live BM MNCs
Diagnosis
Progression
*
D
TNFα Signaling via NFκB
Hypoxia
Apoptosis
UV Response Up
Interferon Response
IL2 STAT5 Signaling
KRAS Signaling Up
Epithelial Mesenchymal Transition
IL6 JAK STAT3 Signaling
MTORC1 Signaling
P value
-log10(P)
E
Scaled Expression
Percent Expressed
Diagnosis
Progression
F
MCL1
Expression Level
Diagnosis
Progression
G
Scaled Expression
Percent Expressed
Diagnosis
Progression
H
RAS wild-type
RAS mutant
Baseline
BP
JUN3
Vinculin
Mcl-1
140 kDa
40 kDa

Figure S7. *RAS* pathway mutated CMML cells upregulate NF-κB survival pathways, including *MCL1*, at BP. Related to Figure 4. (A) Heatmap of the expression levels of the top 5 genes enriched in each of the 21 clusters shown in Fig. 4A. **(B)** UMAP of the distribution of CD34 expression levels across the clusters, as shown in Fig. 4A. Red shading indicates normalized gene expression. Dashed lines indicate MyHPCs. **(C)** Frequency of $Lin^{-}CD34^{+}$ cells in MNCs from *RAS* mutant CMML BM samples sequentially collected at diagnosis and BP after HMA therapy failure (n=9). Statistical significance was calculated using a paired two-tailed Student's t-test (*P <0.05). **(D)** Pathway enrichment analysis of the genes that were significantly upregulated in *RAS* mutant MyHPCs at the time of BP compared with those at diagnosis (adjusted $P \leq 0.05$). The top 10 hallmark gene sets are shown. **(E)** Dot plots of genes belonging to the NF-κB signaling pathway that were significantly upregulated in CMML MyHPCs at BP compared with those at diagnosis (adjusted $P \leq 0.05$). The scaled expression represents z scores across conditions. **(F)** Violin plots of *MCL1* expression levels of *RAS* pathway mutant CMML MyHPCs at diagnosis and BP (adjusted $P = 1.12 \times 10^{-15}$). **(G)** Dot plots of genes belonging to the NF-κB signaling pathway that were significantly upregulated in *RAS* pathway mutant CMML monocytes at BP compared with those at diagnosis (adjusted $P \leq 0.05$). The scaled expression represents z scores across conditions. **(H)** Western blot analysis of MCL1 expression levels in $CD34^{+}$ BM cells isolated from CMML patients at baseline (*RAS* pathway wild-type, n=3; *RAS* pathway mutant, n=3) or at BP (*RAS* pathway wild-type, n=3; *RAS* pathway mutant, n=2). Vinculin was used as a loading control. JJN3 cells are shown as positive controls. The numbers above each case correspond to the patient's UPN (as detailed in Supplementary Table S3).

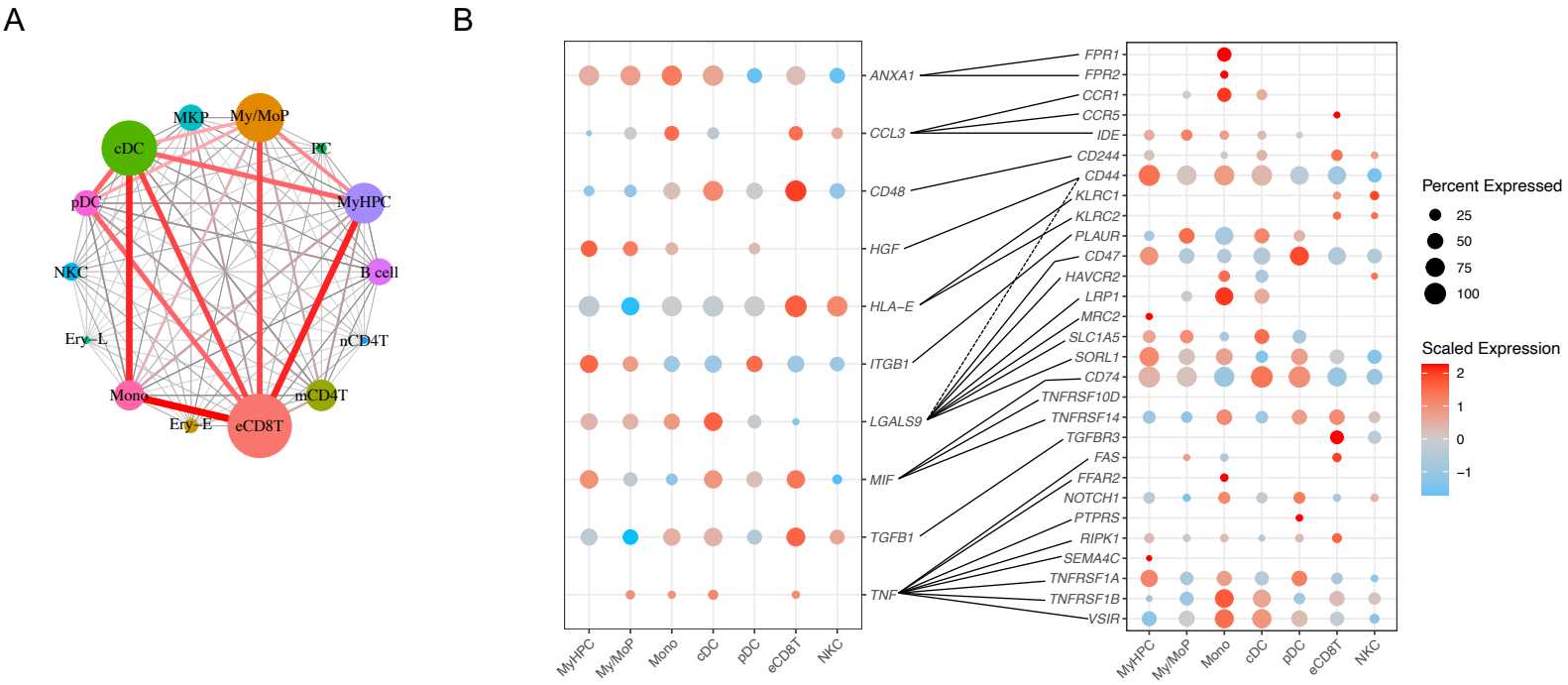

Figure S8. *RAS* pathway mutated CMML MNCs at BP exacerbate the cellular communication networks observed at the time of diagnosis . Related to Figure 4. (A) Connectome web analysis of interactions that were significantly increased in BM MNCs from *RAS* pathway mutant CMML patients at BP compared to those at the time of diagnosis. The vertex (i.e., colored cell node) size is proportional to the number of interactions to and from each cell type, and the thickness of each connecting line is proportional to the number of interactions between 2 nodes. **(B)** Dot plots showing the most significant ligand- (left) to-receptor (right) interactions that were gained in MNCs from *RAS* pathway mutant CMML at diagnosis compared with those at BP (adjusted $P \leq 0.05$). Lines represent connections between ligands and their corresponding receptors. Color saturation indicates the level of gene expression. Dot size indicates the percentage of each cell type expressing the gene. The scaled expression represents z scores across conditions.

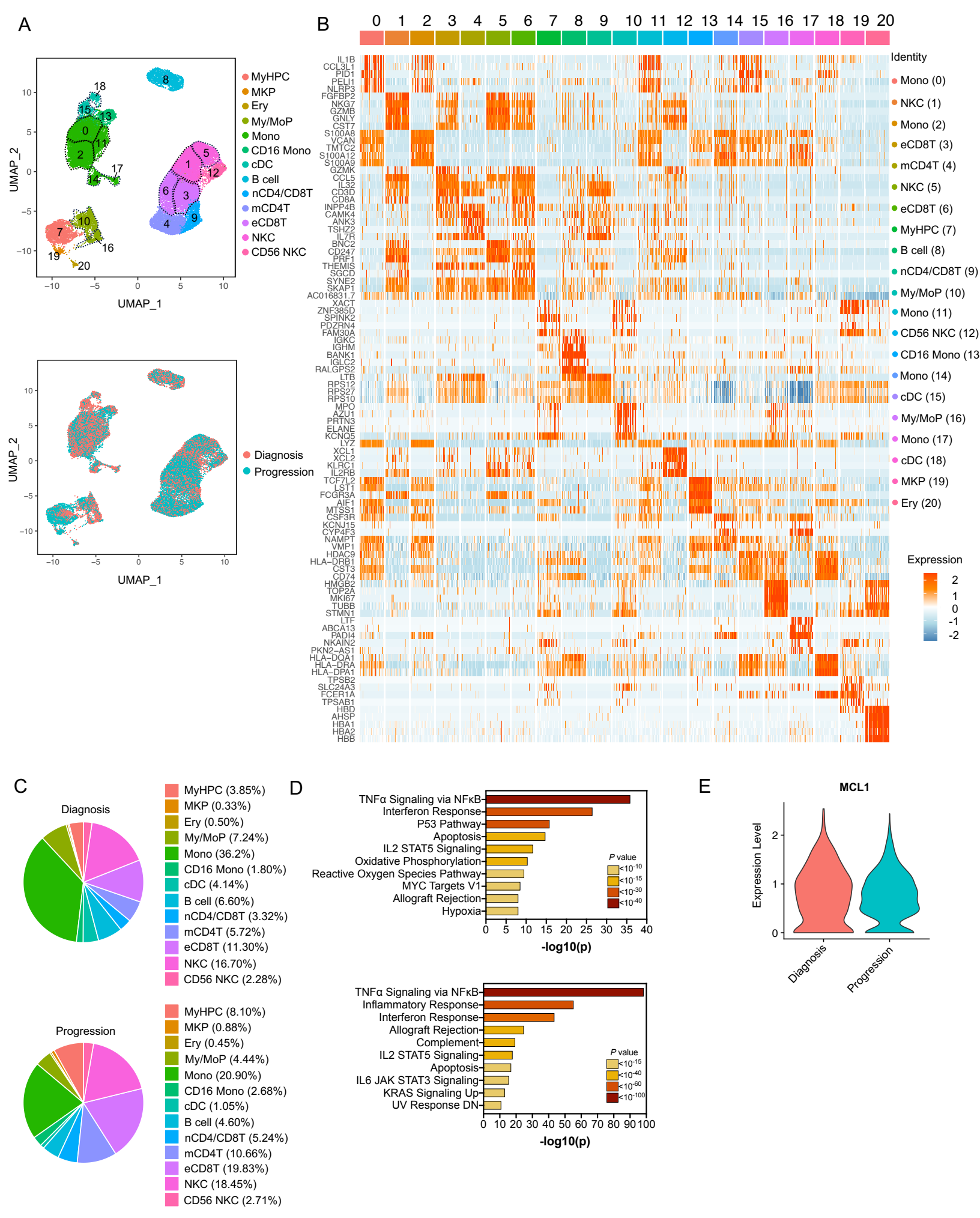
A
UMAP_1
UMAP_2
MyHPC
MKP
Ery
My/MoP
Mono
CD16 Mono
cDC
B cell
nCD4/CD8T
mCD4T
eCD8T
NKC
CD56 NKC
Diagnosis
Progression
B
Identity
Mono (0)
NKC (1)
Mono (2)
eCD8T (3)
mCD4T (4)
NKC (5)
eCD8T (6)
MyHPC (7)
B cell (8)
nCD4/CD8T (9)
My/MoP (10)
Mono (11)
CD56 NKC (12)
CD16 Mono (13
Mono (14)
cDC (15)
My/MoP (16)
Mono (17)
cDC (18)
MKP (19)
Ery (20)
Expression
C
Diagnosis
MyHPC (3.85%)
MKP (0.33%)
Ery (0.50%)
My/MoP (7.24%)
Mono (36.2%)
CD16 Mono (1.80%)
cDC (4.14%)
B cell (6.60%)
nCD4/CD8T (3.32%)
mCD4T (5.72%)
eCD8T (11.30%)
NKC (16.70%)
CD56 NKC (2.28%)
Progression
MyHPC (8.10%)
MKP (0.88%)
Ery (0.45%)
My/MoP (4.44%)
Mono (20.90%)
CD16 Mono (2.68%)
cDC (1.05%)
B cell (4.60%)
nCD4/CD8T (5.24%)
mCD4T (10.66%)
eCD8T (19.83%)
NKC (18.45%)
CD56 NKC (2.71%)
D
TNFα Signaling via NFκB
Interferon Response
P53 Pathway
Apoptosis
IL2 STAT5 Signaling
Oxidative Phosphorylation
Reactive Oxygen Species Pathway
MYC Targets V1
Allograft Rejection
Hypoxia
P value
-log10(p)
TNFα Signaling via NFκB
Inflammatory Response
Interferon Response
Allograft Rejection
Complement
IL2 STAT5 Signaling
Apoptosis
IL6 JAK STAT3 Signaling
KRAS Signaling Up
UV Response DN
P value
-log10(p)
E
MCL1
Expression Level
Diagnosis
Progression

Figure S9. *RAS* pathway wildtype CMML cells do not upregulate MCL1-driven antiapoptotic responses at BP. Related to Figure 4. **(A)** UMAP of scRNA-seq data for pooled single MNCs isolated from 3 BM samples isolated from *RAS* pathway wild-type CMML patients at diagnosis (n=16,070) and BP after HMA therapy failure (n=17,747). Each dot represents one cell. Different colors represent the cluster cell type identity (top) or sample origin (bottom). MyHPC, myeloid hematopoietic progenitor cells; MKP, megakaryocytic progenitor cells; Ery, erythroid precursors; My/MoP, myelo/monocytic progenitors; Mono, monocytes; CD16 Mono, $CD16^+$ non-classical monocytes; cDC, classical dendritic cells; B cell, B lymphocytes; nCD4/CD8T, naïve $CD4^+$, and $CD8^+$ T cells; mCD4T, memory $CD4^+$ T cells; eCD8T, effector $CD8^+$ T cells; NKC, natural killer cells; CD56 NKC, $CD56^+$ natural killer cells. Dashed lines indicate single clusters in each cell type population. **(B)** Heatmap of the expression levels of the top 5 genes enriched in each of the 21 clusters shown in Supplementary Fig. S9A. **(C)** Distribution of MNC populations at diagnosis (top) and BP (bottom) among the clusters shown in Fig. S9A. **(D)** Pathway enrichment analysis of the genes that were significantly upregulated in MyHPCs (top) and monocytes (bottom) from *RAS* pathway wild-type CMML at the time of BP compared with those at diagnosis (adjusted $P \leq 0.05$). The top 10 hallmark gene sets are shown. **(E)** Violin plots of *MCL1* expression levels in *RAS* pathway wild-type CMML MyHPCs at diagnosis and BP (adjusted P = no significant differences).

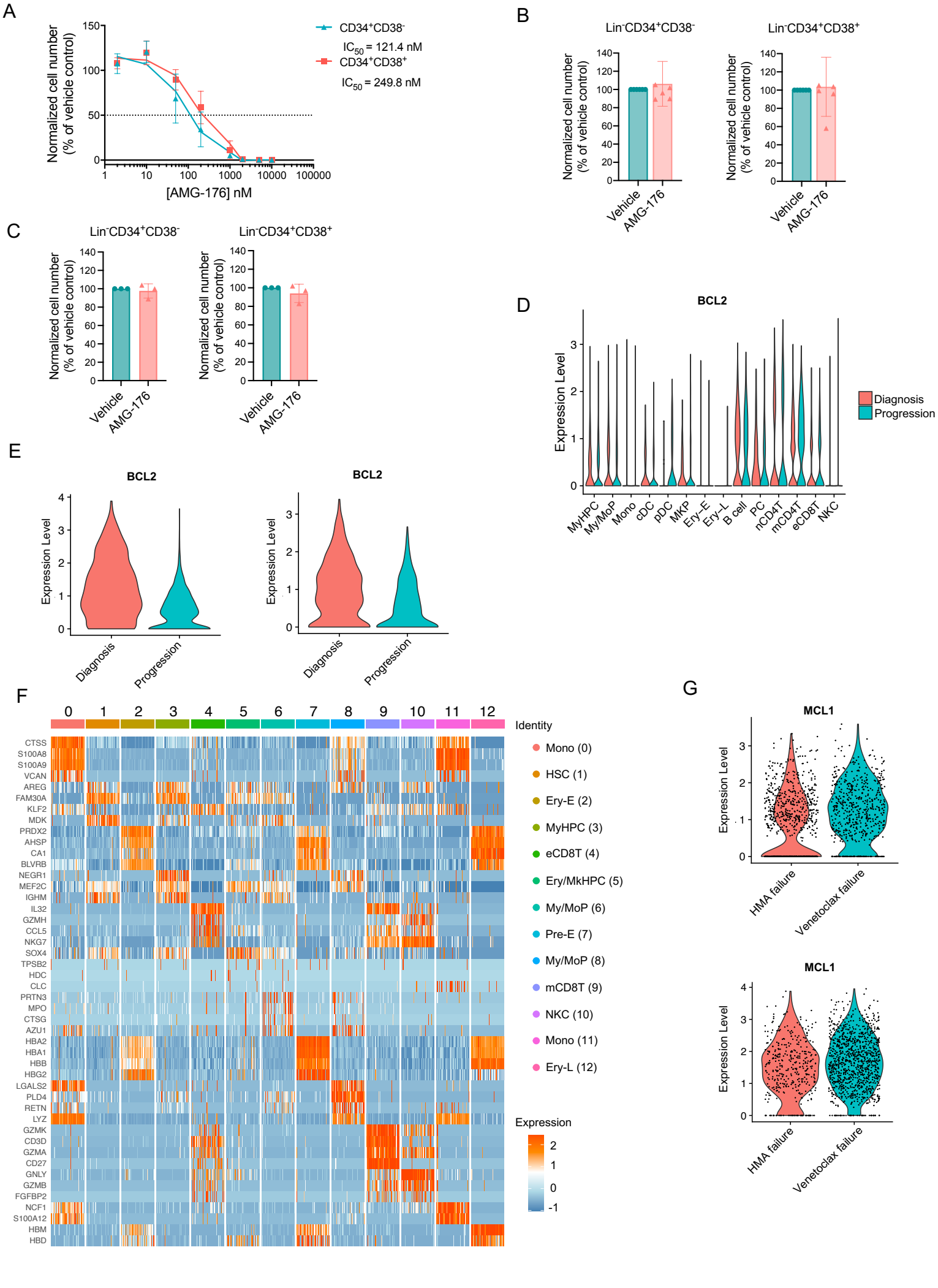
A
Normalized cell number (% of vehicle control)
[AMG-176] nM
CD34+CD38-
IC50 = 121.4 nM
CD34+CD38+
IC50 = 249.8 nM
B
Lin-CD34+CD38-
Lin-CD34+CD38+
Vehicle
AMG-176
C
D
BCL2
Expression Level
Diagnosis
Progression
MyHPC
My/MoP
Mono
cDC
pDC
MKP
Ery-E
Ery-L
B cell
PC
nCD4T
mCD4T
eCD8T
NKC
E
F
Identity
Mono (0)
HSC (1)
Ery-E (2)
MyHPC (3)
eCD8T (4)
Ery/MkHPC (5)
My/MoP (6)
Pre-E (7)
My/MoP (8)
mCD8T (9)
NKC (10)
Mono (11)
Ery-L (12)
Expression
G
MCL1
HMA failure
Venetoclax failure

Figure S10. *RAS* pathway mutated CMML cells, but not *RAS* pathway wildtype CMML cells, rely on *MCL1* overexpression to maintain their survival at BP. Related to Figure 4. (A) Number of live cultured $Lin^{-}CD34^{+}CD38^{-}$ and $Lin^{-}CD34^{+}CD38^{+}$ cells from HD BM samples (n=2) after 48 hours of treatment with AMG-176. Lines represent means ± SEMs. **(B)** Number of live $Lin^{-}CD34^{+}CD38^{-}$ HSCs and $Lin^{-}CD34^{+}CD38^{+}$ MyHPCs from *RAS* pathway mutant CMML patients at diagnosis and after treatment with vehicle or AMG-176 (n=6, 20nM) for 48 hours. Lines represent means ± SDs. A paired two-tailed Student t-test revealed no significant differences. **(C)** Number of live $Lin^{-}CD34^{+}CD38^{-}$ HSCs and $Lin^{-}CD34^{+}CD38^{+}$ MyHPCs from *RAS* pathway wild-type CMML patients at BP after HMA failure and after treatment with vehicle or AMG-176 (n=4, 20nM) for 48 hours. Lines represent means ± SDs. A paired two-tailed Student t-test revealed no significant differences. **(D)** Violin plots of *BCL2* expression levels across each *RAS* pathway mutant CMML MNC population at diagnosis compared with those at BP (no significant difference was detected). **(D)** Violin plots of *BCL2* expression levels in MyHPCs (left) and My/MoPs (right) from *RAS* pathway wild-type CMML at diagnosis compared with those at BP (adjusted $P = 5.45 \times 10^{-54}$ and 1.13×10^{-24}, respectively). **(F)** Heatmap of the expression levels of the top 5 genes enriched in each of the 13 clusters shown in Fig. 4E. **(G)** Violin plots of *MCL1* expression levels in *RAS* pathway mutant MyHPCs (top) and My/MoPs (bottom) at the time of BP after HMA therapy failure compared with those at venetoclax failure (adjusted $P = 1.12 \times 10^{-15}$ and no significant difference, respectively).